Characterization of the polarized endothelial secretome

Haoche Wei[*,†], Ananthalakshmy Sundararaman[†], Emily Dickson[†], Lewis Rennie-Campbell[†], Eloise Cross[†], Kate J. Heesom[†] and Harry Mellor[†,1]

[*]Key Laboratory of Bio-Resource and Eco-Environment of Ministry of Education, Centre for Growth, Metabolism and Aging, College of Life Sciences, Sichuan University, Chengdu, China; and [†]School of Biochemistry, Biomedical Sciences Building, Faculty of Life Sciences, University of Bristol, Bristol BS8 1TD.

[1]Corresponding author:

Professor Harry Mellor

School of Biochemistry,
Biomedical Sciences Building,
University of Bristol,
Bristol BS8 1TD, UK

email: h.mellor@bristol.ac.uk
tel: +44 (0)117 3312174
fax: +44 (0)117 3312168

Running title: Characterization of the polarized endothelial secretome

Abbreviations: Ang2; angiopoietin-2, EC; endothelial cell, ECM; extracellular matrix, EV; extracellular vesicle, FGF; fibroblast growth factor, HUVEC; human umbilical cord ECs, IGF-1; insulin-like growth factor-1, Tsp1; thrombospondin-1.

ABSTRACT

Endothelial cells form an active barrier between the circulation and the body. In addition to controlling transport of molecules between these two compartments, the endothelium is a major secretory organ – releasing proteins both into the circulation and into the vascular matrix. While it is clearly important that proteins are correctly sorted into these two spaces, we currently know little of the polarization of this secretion or how it is controlled. Here we present an optimized system for the analysis of polarized secretion and show that it allows the derivation of deep, robust proteomes from small numbers of primary endothelial cells. We present the first endothelial apical and basolateral secreted proteomes, demonstrating that endothelial cells polarize the secretion of extracellular vesicle cargoes to the apical surface. Conversely, we find that protein secretion at the basolateral surface is focused on components of the extracellular matrix. Finally, we examine the role of liprin-α1 in secretion towards the basolateral compartment and identify a subset of extracellular matrix components that share this route with fibronectin.

Keywords: Endothelial cell, secretion, extracellular matrix, polarization, intracellular traffic.

INTRODUCTION

Endothelial cells (ECs) in a healthy endothelium form a highly polarized monolayer, with their apical (luminal) surface facing the blood space, and their basolateral (abluminal) surface facing the vascular matrix (1). ECs are secretory cells, and protein secretion is a critical part of EC function (2). ECs must secrete extracellular matrix (ECM) components to form the basal lamina, the specialized layer that underlies ECs in stable vessels (3). ECs must also secrete a range of paracrine, autocrine, and endocrine factors that mediate multiple aspects of EC function. These molecules affect vascular tone, proliferation of ECs and vascular smooth muscle cells, EC-leukocyte interactions, platelet adhesion, coagulation, inflammation, and permeability (2, 4).

To carry out these specialized secretory functions, ECs contain specialized adaptions to the generalized intracellular trafficking pathways. ECs are unique in producing Weibel−Palade

bodies; a specialized secretory organelle which mediates the controlled secretion of von Willebrand Factor during thrombosis and hemostasis (5). They also have abundant caveolae; specialized endocytic carriers that mediate transcytosis of albumin and associated molecules across the endothelial layer (6). There is evidence that different EC subtypes have different secretory capacities, depending on their location in the vasculature (2). Additionally, recent work has shown that ECs from different tissue beds secrete tissue-specific combinations of angiocrine factors to mediate tissue-specific paracrine regulation of tissue homeostasis and regeneration (7).

Despite the obvious importance of proteins secretion to EC function, we are only beginning to understand the EC proteome and the mechanisms controlling EC secretion. The first comprehensive proteomic analysis of secreted EC proteins was carried out with human umbilical vein ECs (HUVEC); the most widely studied EC subtype. This identified 374 secreted proteins, ranging from components of the ECM through to angiocrine factors (8). Subsequent proteomic studies have examined how HUVEC protein secretion changes in response to proinflammatory stimuli (9, 10), proangiogenic stimuli (10, 11) and to shear stress (12). Taken together, these studies are beginning to uncover how dynamic regulation matches the EC secretome to EC function.

To date, all proteomic analysis of EC secretion has been on the total secreted proteome, and we know little of the polarity of secretion and the differences between the proteins secreted into the blood and tissue spaces. Early studies showed that ECs secrete more protein to the basolateral space than the apical space (14). The secretion of cellular fibronectin, an important component of the vascular matrix, was shown to be polarized to the basolateral surface (13, 14). The growth factor PDGFβ is also secreted to the basolateral space, allowing for the regulation of mural cell recruitment and proliferation (15). Similarly, the secretion of endothelin-1, a potent regulator of vascular tone, is also highly polarized to the basolateral surface. Endothelin-1 acts on vascular smooth muscle cells of the vessel wall to drive vasoconstriction and this polarized secretion allows localized targeting of these cells (16). Conversely, release of the proinflammatory chemokines IL-6 and TNF- α is highly polarized to the apical space, allowing these mediators to reach more distant tissues via the blood (17). In some cases, ECs are able to control the polarity

of secretion dependent on context; releasing von Willebrand Factor as a low molecular weight form constitutively from their basolateral surface, but as a multimerized form from the apical surface on activation. The basolaterally-secreted von Willebrand Factor forms a reservoir of collagen-bound subendothelial protein, whereas the apically-secreted multimerized factor promotes platelet binding and thrombosis (18). The ability to control the routing of von Willebrand Factor in this way allows for the proper control of thrombosis and hemostasis.

Clearly, it is critical that ECs are able to direct proteins to the appropriate cell surface; however, we currently know little of how this is regulated, or even which proteins are secreted into the vascular matrix and which to the circulation. Here we present the first proteomic analysis of polarized secretion in ECs, defining the apical and basolateral proteomes. We show that ECs polarize secretion of vascular matrix components to the basolateral surface, including not only the matrix proteins themselves, but also the wide range of protein factors responsible for matrix remodeling. In contrast, we show the apical EC proteome is primarily composed of proteins secreted through the extracellular vesicle pathway. Finally, we show that this methodology is well-suited to the investigation of EC secretion mechanisms by identifying a subset of vascular matrix proteins whose polarized secretion is controlled by the cytoskeletal linker protein liprin-α1.

MATERIALS AND METHODS

Reagents and antibodies

Unless stated, all reagents were from Sigma-Aldrich (Dorset, UK). A mouse monoclonal antibody to VE-cadherin (clone 55-7H1) was from BD Biosciences (Berkshire, UK); a rabbit polyclonal antibody to ZO-1 (#61-7300) was from ThermoFisher Scientific (Loughborough, UK); a rabbit polyclonal antibody to liprin-α1 (#14175) was from Proteintech (Manchester, UK). Alexa Fluor 488- and 594-conjugated secondary antibodies were from ThermoFisher Scientific.

Cell culture

HUVECs pooled from multiple donors were obtained from Lonza (Basel, Switzerland) and cultured in EGM-2 medium (Lonza). For polarized secretion assays, HUVEC (2×10^5/ml) were plated in Transwell tissue culture inserts with 0.4μm pore size (Millipore; Hertfordshire, UK).

Cells were cultured for 24h in EGM-2 until they formed a continuous monolayer. The cells were then washed, and the medium replaced with HIFA2 medium. To make HIFA2 medium, EGM-2 was prepared without the provided FBS, FGF-2, IGF-1, EGF and VEGF supplements. This was then supplemented with 10ng/ml recombinant human FGF-2 and 20ng/ml recombinant IGF-1 LR3 (R&D Systems, Oxford, UK) to make HIFA2. Cells were allowed to condition the medium for a further 48h before the medium was collected for analysis.

Permeability measurements

HUVEC were cultured in Transwell inserts for 24h, as described above. FITC-dextran (40kDa) was added to the top chamber at a final concentration of 1µg/ml. After a further 24h, medium was collected from the bottom chamber and fluorescence measured in a fluorimeter. Permeability of the monolayers to protein was assayed by following the transport of BSA. Cells were cultured in Transwell inserts as described and then fatty-acid free BSA was added to either the top, bottom or both chambers at a final concentration of 0.1µg/ml. After a further 24h, samples of medium were removed and BSA was quantified by densitometry of Coomassie Blue stained SDS-PAGE gels.

Immunofluorescence microscopy

The preparation of cells for immunofluorescence microscopy was carried out as previously described (19). Briefly, cells were fixed in 4% paraformaldehyde in PBS for 15min. The cells were then permeabilized with 0.2% Triton X-100 in PBS for 5min. Cells were then treated with 0.1% freshly-prepared sodium borohydride in PBS for 5min to quench autofluorescence. The cells were washed three times in PBS between each step. The fixed cells were incubated with primary antibodies for 1h in PBS, followed by incubation in secondary antibodies for 45min. Cells were washed three times in PBS between each step. The cells were then incubated with 300nM DAPI for 10min and mounted under Mowiol containing 2.5% (w/v) DABCO as an antifade agent. Confocal microscopy was performed using a Leica SP5 AOBS confocal laser-scanning microscope with an attached Leica DM I6000 inverted microscope. Confocal sections were taken across the z-plane and processed to form a 2D projection representing the full depth of the cells.

Proteomic analysis

Conditioned medium was taken from the top and bottom chambers of the Transwell inserts. The two chambers have different volumes, and the apical-derived medium was adjusted to the volume of the basolateral-derived medium with HIFA2. The two equal volumes (1.3ml) of medium were then concentrated to 20µl using Amicon Ultracel microconcentrators (3kDa cut-off; Millipore, Hertfordshire, UK). Samples were digested with trypsin, labelled with Tandem Mass Tag (TMT) six plex reagents according to the manufacturer's protocol (ThermoFisher Scientific) and the labelled samples pooled. This pooled sample was then evaporated to dryness, resuspended in 5% formic acid and desalted using a SepPak cartridge according to the manufacturer's instructions (Waters, Massachusetts, USA). Eluate from the SepPak cartridge was again evaporated to dryness and resuspended in 1% formic acid prior to analysis by nano-LC MSMS using an Orbitrap Fusion Tribrid Mass Spectrometer, as described previously (20). The raw data files were processed and quantified using Proteome Discoverer software v2.1 (ThermoFisher Scientific) and searched against the UniProt Human database (140,000 entries) using the SEQUEST algorithm. Peptide precursor mass tolerance was set at 10 ppm, and MS/MS tolerance was set at 0.6 Da. Search criteria included the oxidation of methionine (+15.9949) as a variable modification and carbamidomethylation of cysteine (+57.0214) and the addition of the TMT mass tag (+229.163) to peptide N-termini and lysine as fixed modifications. Searches were performed with full tryptic digestion and a maximum of two missed cleavage events were allowed. The reverse database search option was enabled, and all data were filtered to satisfy false discovery rate (FDR) of 5%.

siRNA transfection

Three siRNA oligonucleotide duplexes targeting liprin-α1 were synthesized by Origene Technologies (Herford, Germany): LP01; 5'-AGUUUAGACCAAAGGACAUUCGUGG-3', LP02; 5'-GCAUGACCUCAAUGAUAAACUUGAA-3', LP03; 5'-CCAAGGUACAAACUCUUAAUGAGCA-3'. A control siRNA duplex (#SR30004) was also from Origene. Transfection of HUVEC with siRNAs was performed using Genefector transfection reagent (Venn Nova Inc, Florida, US), according to the manufacturer's instructions and with a 3h incubation period. Cells were transfected 48h before the termination of experiments.

ELISA

Concentrations of thrombospondin-1, angiopoetin-2 and fibronectin were quantified in conditioned medium using ELISA kits, used according to the manufacturers' instructions (R&D Systems).

SDS-PAGE and western blotting

Proteins were analyzed by SDS-PAGE on 10% polyacrylamide gels. Proteins were transferred to polyvinylidene fluoride membrane for immunoblotting.

Statistical analysis

Analysis of differences between multiple samples was made using one-way ANOVA with Tukey's post hoc test.

RESULTS

Optimization of a polarized endothelial monolayer

We chose HUVEC for our studies; the most widely-used EC subtype, and the cell type used for previous proteomic analyses of total secretion (8-11). To separate the apical and basolateral compartments, we cultured cells in Transwell tissue culture inserts with a 0.4μm pore size. HUVEC monolayers are known to have a relatively high permeability, and we wanted to maximize their barrier function to ensure that secreted proteins could not leak between cells, normalizing their distribution. Commercial endothelial growth medium is optimized for cell proliferation, and many of the components that promote proliferation (serum and growth factors) also promote junctional instability. To optimize the barrier properties of the HUVEC, we measured the contribution of each of the media supplements. We used the transport of FITC-dextran across the monolayer as a measure of permeability. Removal of serum from the medium significantly improved the barrier function (Fig. 1A). We examined the effects of removing each of the other media supplements in a serum-free background. Removal of hydrocortisone, FGF-2 or IGF-1 significantly disrupted barrier function, whereas the removal of other components had little effect (Fig. 1A). We also examined the effect of addition of forskolin, a small molecule

that raises cellular cAMP and stabilizes EC junctions (21). Forskolin treatment gave no further improvement over the removal of serum (Fig. 1A).

We formulated an optimized serum-free medium comprising EGM-2 base medium supplemented with hydrocortisone, IGF-1, FGF-2 and ascorbate (HIFA). While ascorbate was not required for optimal barrier function, its presence is important for normal collagen processing. In preparation for proteomic analysis, we cultured EC monolayers on Transwell inserts in HIFA for 48h and then concentrated the medium from the apical and basolateral chambers. We analyzed the protein content of this medium by SDS-PAGE and saw a strong band at approximately 67 kDa, consistent with albumin contamination (Fig. 1B). The same band was present in concentrated HIFA medium that had not been exposed to cells, suggesting that this contamination derived from the media supplements (Fig. 1B). Further analysis showed that the FGF-2 and IGF-1 supplements provided with the medium were the source of this band, and of several other contaminating proteins (Fig. 1B). We replaced these with purified recombinant growth factors, to produce a medium with negligible protein content (Fig. 1B). This formulation was termed HIFA2, and a full description of the formulation is given in the Methods section. HIFA2 gave a 42% improvement to barrier function compared to the original EGM-2 (Fig. 1A). HUVEC cultured in EGM-2 displayed the characteristic 'zipper' morphology of unstable cell-cell junctions, whereas cells cultured in HIFA2 had more linear, continuous junctions (Fig. 1C). To determine whether these junctions were stable enough to maintain an asymmetric distribution of proteins across the barrier, we incubated cells with exogenous albumin. Addition of albumin to either side of the EC monolayer resulted in transport of only 20% of the protein tracer across the barrier over a 24h period (Fig. 1D). ECs facilitate movement of albumin across the endothelium via transcytosis (22), which will contribute to some of this transport. We concluded that the barrier function of HUVEC cultured in HIFA2 was sufficient for proteomic analysis of polarized secretion.

Proteomic analysis of polarized endothelial cell secretion

Confluent monolayers of HUVEC were transferred to HIFA2 and allowed to condition the medium for 48h. The medium was then collected from the apical and basolateral chambers and concentrated by microfiltration. Tryptic peptides from the samples were subjected to tandem

mass tagging; an isobaric labelling strategy that allows for relative quantitative proteomics (23). Data were collected from three independent experiments. In total, 1552 proteins were identified, of which 382 proteins were detected in all three experiments Fig. 2A. The full dataset is presented in Supplemental Table S1A. Table 1 shows the 5 proteins with the most asymmetric secretion to the apical and basolateral compartments, respectively. Cursory examination of the data showed that the two proteomes are very different. Proteins secreted from the basolateral surface of ECs were largely conventionally secreted proteins and were enriched in components of the extracellular matrix. Proteins secreted from the apical surface were enriched in components of extracellular vesicles. In conventional protein secretion, recognition of a signal peptide at the N-terminus of the peptide allows for its targeting to the endoplasmic reticulum for entry into the secretory pathway. In contrast, secretion via extracellular vesicles involves the packaging of cytosolic proteins into membrane wrappers which are then shed from the cell (24). In endothelial cells, these extracellular vesicles play important roles in long-range intercellular signaling in the vasculature (25, 26). Fig. 2B shows a plot of the 840 proteins that were detected in at least two independent experiments. Secretion of the majority of proteins (90%) was polarized towards the apical surface. We analyzed our secreted proteome to identify conventional soluble secreted proteins, using the VerSeDa database (27). Fig. 2C shows the relative distribution between the apical and basolateral compartments of proteins with a conventional signal peptide and no predicted transmembrane regions. The majority were either polarized towards the basolateral surface or showed no overall polarization. We also interrogated the Matrisome Project database (28) to identify components of the extracellular matrix. ECM proteins showed a similar distribution to the pool of soluble secreted proteins (Fig. 2C), and 55% of the predicted conventionally secreted EC proteins were also identified in the ECM database. For comparison, we determined the relative distribution of protein makers of extracellular vesicles by interrogating the EVpedia database (29). Fig. 2C shows the relative distribution proteins matching to the top 500 human extracellular vesicle (EV) proteins. Secretion of EV proteins was highly polarized to the apical surface, with 97% of EV proteins showing apical polarization.

To validate the proteomic analysis, we selected representative proteins with a clear polarity to their secretion. Thrombospondin-1 (Tsp1) is a component of the vascular matrix that plays

important roles in organization of the ECM and in inhibiting angiogenesis (30). In keeping with this, our proteomic analysis showed that 60% of Tsp1 was secreted to the basolateral compartment. Angiopoietin-2 (Ang2) is a pro-angiogenic factor whose circulating levels are elevated in pathological angiogenesis and in inflammation and sepsis (31). Our proteomic analysis showed that 64% of Ang2 was secreted to the apical compartment. The relative ratio of each protein between the apical and basolateral compartments was determined by ELISA (Fig. 2D). In each case, the ratio determined from the actual concentrations is in good agreement with the ratio estimated by the TMT-based proteomic analysis.

We conclude that there are two major pathways of secretion in ECs, with the conventional secretory pathway delivering ECM components to the vascular matrix and the EV pathway producing signaling intermediates that are released from the apical surface for propagation of long-range signals through the circulation.

Liprin-α1 controls sorting of a subset of ECM proteins to the basolateral surface

Analysis of the proteomic data demonstrated that our optimized TMT-based protocol was capable of generating robust data from small samples of ECs. Currently little is known of the regulation of EC secretion under physiological and pathological conditions and our protocol has the potential to allow for relatively straightforward analysis of perturbations to polarized EC secretion. To explore this, we examined the effects of disrupting one specific aspect of EC secretion. While the mechanisms of polarized secretion in ECs are poorly understood, recent studies have shown that liprin-α1/PPFAI1 controls the delivery of fibronectin to the basolateral face of ECs (32). Fibronectin is the best characterized EC protein in terms of polarized secretion and is delivered mainly to the basolateral surface in resting ECs (13, 14). We used siRNA mediated silencing to deplete liprin-α1 from ECs, selecting two oligonucleotide duplexes that gave effective suppression of expression (Fig. 3A). We then tested whether silencing of liprin-α1 affected EC permeability – which would potentially confound the assay by allowing secreted proteins to leak across the EC monolayer. Neither of the siRNAs significantly affected permeability (Fig. 3B). To confirm the effect of liprin-α1 on fibronectin secretion, we measured the concentration of fibronectin in the apical and basolateral compartments by ELISA. As previously reported, fibronectin was secreted predominantly to the basolateral surface (Fig. 3C).

Interestingly, silencing of liprin-α1 had no effect on the apical secretion of fibronectin, but significantly inhibited its delivery to the basolateral compartment (Fig. 3C). We then performed a full proteomic analysis of secretion from ECs silenced for liprin-α1 to identify other proteins that might also depend on liprin-α1 for their correct secretion. The full dataset is presented in Supplemental Table S1B. The vast majority of proteins were unaffected by liprin-α1 depletion; however, a subset of proteins showed significant disruption to their normal polarity of secretion (Fig. 3D). We were interested in proteins that were normally secreted to the basolateral surface, but which then shifted towards apical secretion on depletion of liprin-α1 – such proteins potentially share the same mechanism of polarized secretion as fibronectin. Table 2 shows the four most shifted proteins, with fibronectin as a comparison. All are conventionally secreted proteins, and all showed a more dramatic reduction of basolateral polarization than fibronectin itself. Interestingly, three of these proteins are ECM components that play important roles in the regulation and remodeling of the vascular matrix. The secreted form of dystroglycan-1 binds laminin, agrin and perlecan to promote organization of the basement lamina (33). Lysyl oxidase controls the maturation of the vascular matrix and binds directly to fibronectin. Reduced matrix deposition of lysyl oxidase is associated with endothelial dysfunction, whereas upregulation of this enzyme can induce neointimal thickening in atherosclerosis (34). Multimerin-2 is an EC-specific ECM protein that also interacts with fibronectin and is required for remodeling of secreted fibronectin into fibrils (35). Intriguingly, both multimerin-2 and dystroglycan-1 interact with the pro-angiogenic lectin CD93 in ECs (35, 36), suggesting that the potential for co-trafficking and co-complex formation. Finally, phospholipid transfer protein (PLTP) is a regulator of cholesterol efflux from ECs through its role in HDL formation. Increases in circulating PTLP are linked to atherogenesis (37), suggesting that disruption of the normal polarity of secretion in this way would lead to pathogenesis.

In addition to proteins that mimicked the loss of basolateral polarity seen with fibronectin, we also observed a subset of proteins that showed re-routing in the reverse direction – i.e. which lost strong apical polarization (Fig. 3E). Again, these were all conventionally-secreted ECM proteins. We saw re-routing of both subunits of collagen I to the basolateral surface. Intriguingly, we also saw re-routing of reticulocalbin-3 – a negative regulator of collagen I production with links to cardiac fibrosis (38). The fourth protein was ECM1 – a protein with an

organizing function for the basement lamina and another interacting partner of fibronectin (39). The rerouting of collagen I towards the basolateral surface in response to perturbation of fibronectin secretion implies the existence of cross-talk between those two intracellular sorting pathways and reactive regulation of the composition of the vascular matrix.

DISCUSSION

In an adult human, the endothelial cell (EC) surface is composed approximately of 10-60 trillion cells, weighs approximately 1kg, and covers a surface area of 1-7 m^2 (40). This makes the endothelium one of the largest secretory organs in the body, and yet we still know relatively little about the proteins that it secretes, or how this secretion is regulated. ECs form the interface between to very distinct compartments – the circulation and the vascular matrix. It is clear that polarized secretion allows for the correct proteins to be delivered to the correct destination; however, we currently know the destinations of only a handful of EC proteins. Here we present the first polarized EC secretome and demonstrate marked differences in secretion at the two EC surfaces. We show that conventionally secreted proteins are distributed between the apical and basolateral surfaces, with a strong enrichment for ECM components in the basolateral proteome. We find that secretion of extracellular vesicle cargoes is strongly polarized to the apical surface.

It is clear that ECs have mechanisms to allow for the sorting of proteins to the correct compartment; however, our understanding of these mechanisms is extremely limited. We examined one of these mechanisms – the role of liprin-α1 in the sorting of fibronectin to the basolateral surface. Polarized sorting of fibronectin appears to be a distinct function of ECs (41) and liprin-α1 mediates sorting of a complex of soluble fibronectin and activated integrin α5ß1 to the basolateral face of ECs (32). We used our platform to determine if other cargoes were sorted through this route and identified 4 additional proteins that depended on liprin-α1 for effective delivery to the basolateral compartment. Interestingly, three of these are known to bind directly fibronectin, or to binding partners of fibronectin. Fibronectin is known to be targeted to specific ECM contact sites at the basolateral surface (35). Co-trafficking of these proteins through the liprin-α1 pathway would ensure their co-location at the EC/ECM interface. These findings demonstrate the ability of this approach to dissect the mechanism of polarized protein sorting in

ECs. The fact that the majority of EC proteins are not affected by liprin-α1 depletion tells us that there must be further, unknown mechanisms of polarized trafficking to be discovered.

Going forward, our proteomic platform offers three advantages for the analysis of EC secretion. First, the improved barrier function allows the asymmetric distribution of proteins to be maintained for long periods after secretion, aiding analysis. Second, the optimized medium formulation is essentially protein-free, which allows significant concentration of the medium prior to analysis, increasing the sensitivity of detection. Third, our method allows for the derivation of deep, robust proteomes from small samples (c.a. 10^5 primary cells), allowing for the analysis of samples from specialized conditions and/or endothelial subtypes. Important problems to address include the changes to the vascular ECM composition seen in various vascular diseases (42), which may involve dysregulation of polarized secretion. This method is also amenable to the study of the differences in secretion between different vascular beds – and the consequent unique homeostatic and regenerative contributions that these different ECs make to their tissues. In both cases, the small sample size required will allow for the study of rare or difficult to obtain samples.

ACKNOWLEDGEMENTS

Haoche Wei was supported by a scholarship from the Chinese Scholarship Council. Ananthalakshmy Sundararaman was supported by a project grant from the British Heart Foundation.

AUTHOR CONTRIBUTIONS

H.W. performed most of the experimental work, with assistance from E.D, E.C. and A.S. for ELISA assays. K.J.H. performed the proteomic analysis and provided specialist input to the experimental design for that work. L.R.-C. and H.M. performed the bioinformatic analysis of the proteomic data. H.M. conceived the study and wrote the manuscript.

REFERENCES

1. Galley, H. F., and Webster, N. R. (2004) Physiology of the endothelium. *Br J Anaesth* **93**, 105-113
2. Neumüller, J., and Ellinger, A. (2008) Secretion and endocytosis in endothelial cells. In *The Golgi Apparatus* (Mironov, A. A., and Pavelka, M., eds), Springer, Vienna
3. Yurchenco, P. D. (2011) Basement membranes: cell scaffoldings and signaling platforms. *Cold Spring Harb Perspect Biol* **3**
4. Muniyappa, R., and Sowers, J. R. (2013) Role of insulin resistance in endothelial dysfunction. *Rev Endocr Metab Disord* **14**, 5-12
5. McCormack, J. J., Lopes da Silva, M., Ferraro, F., Patella, F., and Cutler, D. F. (2017) Weibel-Palade bodies at a glance. *J Cell Sci* **130**, 3611-3617
6. Ghitescu, L., Fixman, A., Simionescu, M., and Simionescu, N. (1986) Specific binding sites for albumin restricted to plasmalemmal vesicles of continuous capillary endothelium: receptor-mediated transcytosis. *J Cell Biol* **102**, 1304-1311
7. Augustin, H. G., and Koh, G. Y. (2017) Organotypic vasculature: From descriptive heterogeneity to functional pathophysiology. *Science* **357**
8. Tunica, D. G., Yin, X., Sidibe, A., Stegemann, C., Nissum, M., Zeng, L., Brunet, M., and Mayr, M. (2009) Proteomic analysis of the secretome of human umbilical vein endothelial cells using a combination of free-flow electrophoresis and nanoflow LC-MS/MS. *Proteomics* **9**, 4991-4996
9. Bal, G., Kamhieh-Milz, J., Sterzer, V., Al-Samman, M., Debski, J., Klein, O., Kamhieh-Milz, S., Bhakdi, S., and Salama, A. (2013) Proteomic profiling of secreted proteins for the hematopoietic support of interleukin-stimulated human umbilical vein endothelial cells. *Cell Transplant* **22**, 1185-1199
10. Mohr, T., Haudek-Prinz, V., Slany, A., Grillari, J., Micksche, M., and Gerner, C. (2017) Proteome profiling in IL-1β and VEGF-activated human umbilical vein endothelial cells delineates the interlink between inflammation and angiogenesis. *PLoS One* **12**, e0179065
11. Zanivan, S., Maione, F., Hein, M. Y., Hernandez-Fernaud, J. R., Ostasiewicz, P., Giraudo, E., and Mann, M. (2013) SILAC-based proteomics of human primary endothelial cell morphogenesis unveils tumor angiogenic markers. *Molecular & cellular proteomics : MCP* **12**, 3599-3611
12. Burghoff, S., and Schrader, J. (2011) Secretome of human endothelial cells under shear stress. *J Proteome Res* **10**, 1160-1169
13. Kowalczyk, A. P., Tulloh, R. H., and McKeown-Longo, P. J. (1990) Polarized fibronectin secretion and localized matrix assembly sites correlate with subendothelial matrix formation. *Blood* **75**, 2335-2342
14. Unemori, E. N., Bouhana, K. S., and Werb, Z. (1990) Vectorial secretion of extracellular matrix proteins, matrix-degrading proteinases, and tissue inhibitor of metalloproteinases by endothelial cells. *J. Biol. Chem.* **265**, 445-451
15. Zerwes, H. G., and Risau, W. (1987) Polarized secretion of a platelet-derived growth factor-like chemotactic factor by endothelial cells in vitro. *J Cell Biol* **105**, 2037-2041
16. Wagner, O. F., Christ, G., Wojta, J., Vierhapper, H., Parzer, S., Nowotny, P. J., Schneider, B., Waldhäusl, W., and Binder, B. R. (1992) Polar secretion of endothelin-1 by cultured endothelial cells. *J Biol Chem* **267**, 16066-16068

17. Verma, S., Nakaoke, R., Dohgu, S., and Banks, W. A. (2006) Release of cytokines by brain endothelial cells: A polarized response to lipopolysaccharide. *Brain Behav Immun* **20**, 449-455
18. Lopes da Silva, M., and Cutler, D. F. (2016) von Willebrand factor multimerization and the polarity of secretory pathways in endothelial cells. *Blood* **128**, 277-285
19. Richards, M., Hetheridge, C., and Mellor, H. (2015) The Formin FMNL3 Controls Early Apical Specification in Endothelial Cells by Regulating the Polarized Trafficking of Podocalyxin. *Curr. Biol.* **25**, 2325-2331
20. Hawksworth, J., Satchwell, T. J., Meinders, M., Daniels, D. E., Regan, F., Thornton, N. M., Wilson, M. C., Dobbe, J. G., Streekstra, G. J., Trakarnsanga, K., Heesom, K. J., Anstee, D. J., Frayne, J., and Toye, A. M. (2018) Enhancement of red blood cell transfusion compatibility using CRISPR-mediated erythroblast gene editing. *EMBO Mol Med* **10**
21. Noda, K., Zhang, J., Fukuhara, S., Kunimoto, S., Yoshimura, M., and Mochizuki, N. (2010) Vascular endothelial-cadherin stabilizes at cell-cell junctions by anchoring to circumferential actin bundles through alpha- and beta-catenins in cyclic AMP-Epac-Rap1 signal-activated endothelial cells. *Mol Biol Cell* **21**, 584-596
22. Fung, K. Y. Y., Fairn, G. D., and Lee, W. L. (2018) Transcellular vesicular transport in epithelial and endothelial cells: Challenges and opportunities. *Traffic* **19**, 5-18
23. Zhang, L., and Elias, J. E. (2017) Relative Protein Quantification Using Tandem Mass Tag Mass Spectrometry. *Methods Mol Biol* **1550**, 185-198
24. D'Souza-Schorey, C., and Schorey, J. S. (2018) Regulation and mechanisms of extracellular vesicle biogenesis and secretion. *Essays Biochem* **62**, 125-133
25. Todorova, D., Simoncini, S., Lacroix, R., Sabatier, F., and Dignat-George, F. (2017) Extracellular Vesicles in Angiogenesis. *Circ Res* **120**, 1658-1673
26. Hromada, C., Mühleder, S., Grillari, J., Redl, H., and Holnthoner, W. (2017) Endothelial Extracellular Vesicles-Promises and Challenges. *Front Physiol* **8**, 275
27. Cortazar, A. R., Oguiza, J. A., Aransay, A. M., and Lavín, J. L. (2017) VerSeDa: vertebrate secretome database. *Database (Oxford)* **2017**
28. Chautard, E., Ballut, L., Thierry-Mieg, N., and Ricard-Blum, S. (2009) MatrixDB, a database focused on extracellular protein-protein and protein-carbohydrate interactions. *Bioinformatics* **25**, 690-691
29. Kim, D. K., Lee, J., Kim, S. R., Choi, D. S., Yoon, Y. J., Kim, J. H., Go, G., Nhung, D., Hong, K., Jang, S. C., Kim, S. H., Park, K. S., Kim, O. Y., Park, H. T., Seo, J. H., Aikawa, E., Baj-Krzyworzeka, M., van Balkom, B. W., Belting, M., Blanc, L., Bond, V., Bongiovanni, A., Borràs, F. E., Buée, L., Buzás, E. I., Cheng, L., Clayton, A., Cocucci, E., Dela Cruz, C. S., Desiderio, D. M., Di Vizio, D., Ekström, K., Falcon-Perez, J. M., Gardiner, C., Giebel, B., Greening, D. W., Gross, J. C., Gupta, D., Hendrix, A., Hill, A. F., Hill, M. M., Nolte-'t Hoen, E., Hwang, D. W., Inal, J., Jagannadham, M. V., Jayachandran, M., Jee, Y. K., Jørgensen, M., Kim, K. P., Kim, Y. K., Kislinger, T., Lässer, C., Lee, D. S., Lee, H., van Leeuwen, J., Lener, T., Liu, M. L., Lötvall, J., Marcilla, A., Mathivanan, S., Möller, A., Morhayim, J., Mullier, F., Nazarenko, I., Nieuwland, R., Nunes, D. N., Pang, K., Park, J., Patel, T., Pocsfalvi, G., Del Portillo, H., Putz, U., Ramirez, M. I., Rodrigues, M. L., Roh, T. Y., Royo, F., Sahoo, S., Schiffelers, R., Sharma, S., Siljander, P., Simpson, R. J., Soekmadji, C., Stahl, P., Stensballe, A., Stępień, E., Tahara, H., Trummer, A., Valadi, H., Vella, L. J., Wai, S. N., Witwer, K.,

Yáñez-Mó, M., Youn, H., Zeidler, R., and Gho, Y. S. (2015) EVpedia: a community web portal for extracellular vesicles research. *Bioinformatics* **31**, 933-939
30. Zhang, X., and Lawler, J. (2007) Thrombospondin-based antiangiogenic therapy. *Microvasc Res* **74**, 90-99
31. Thurston, G., and Daly, C. (2012) The complex role of angiopoietin-2 in the angiopoietin-tie signaling pathway. *Cold Spring Harb Perspect Med* **2**, a006550
32. Mana, G., Clapero, F., Panieri, E., Panero, V., Böttcher, R. T., Tseng, H. Y., Saltarin, F., Astanina, E., Wolanska, K. I., Morgan, M. R., Humphries, M. J., Santoro, M. M., Serini, G., and Valdembri, D. (2016) PPFIA1 drives active α5β1 integrin recycling and controls fibronectin fibrillogenesis and vascular morphogenesis. *Nat Commun* **7**, 13546
33. Barresi, R., and Campbell, K. P. (2006) Dystroglycan: from biosynthesis to pathogenesis of human disease. *J Cell Sci* **119**, 199-207
34. Rodríguez, C., Martínez-González, J., Raposo, B., Alcudia, J. F., Guadall, A., and Badimon, L. (2008) Regulation of lysyl oxidase in vascular cells: lysyl oxidase as a new player in cardiovascular diseases. *Cardiovasc Res* **79**, 7-13
35. Lugano, R., Vemuri, K., Yu, D., Bergqvist, M., Smits, A., Essand, M., Johansson, S., Dejana, E., and Dimberg, A. (2018) CD93 promotes β1 integrin activation and fibronectin fibrillogenesis during tumor angiogenesis. *J Clin Invest* **128**, 3280-3297
36. Galvagni, F., Nardi, F., Maida, M., Bernardini, G., Vannuccini, S., Petraglia, F., Santucci, A., and Orlandini, M. (2016) CD93 and dystroglycan cooperation in human endothelial cell adhesion and migration adhesion and migration. *Oncotarget* **7**, 10090-10103
37. Albers, J. J., Vuletic, S., and Cheung, M. C. (2012) Role of plasma phospholipid transfer protein in lipid and lipoprotein metabolism. *Biochim Biophys Acta* **1821**, 345-357
38. Martínez-Martínez, E., Ibarrola, J., Fernández-Celis, A., Santamaria, E., Fernández-Irigoyen, J., Rossignol, P., Jaisser, F., and López-Andrés, N. (2017) Differential Proteomics Identifies Reticulocalbin-3 as a Novel Negative Mediator of Collagen Production in Human Cardiac Fibroblasts. *Sci Rep* **7**, 12192
39. Sercu, S., Zhang, L., and Merregaert, J. (2008) The extracellular matrix protein 1: its molecular interaction and implication in tumor progression. *Cancer Invest* **26**, 375-384
40. Cines, D. B., Pollak, E. S., Buck, C. A., Loscalzo, J., Zimmerman, G. A., McEver, R. P., Pober, J. S., Wick, T. M., Konkle, B. A., Schwartz, B. S., Barnathan, E. S., McCrae, K. R., Hug, B. A., Schmidt, A. M., and Stern, D. M. (1998) Endothelial cells in physiology and in the pathophysiology of vascular disorders. *Blood* **91**, 3527-3561
41. Hamidi, H., and Ivaska, J. (2017) Vascular Morphogenesis: An Integrin and Fibronectin Highway. *Curr Biol* **27**, R158-R161
42. Lynch, M., Barallobre-Barreiro, J., Jahangiri, M., and Mayr, M. (2016) Vascular proteomics in metabolic and cardiovascular diseases. *J. Intern. Med.* **280**, 325-338

FIGURE LEGENDS

Fig. 1 Optimization of an endothelial monolayer. *A*) HUVEC were grown in Transwell inserts for 24h to achieve confluence. Medium was then removed and replaced with either complete EGM-2, or EGM-2 lacking various supplements, as indicated. FITC-dextran was added to the top chamber and its passage across the monolayer was measured by fluorimetry of the medium from the bottom chamber after 24h. Hydrocortisone, FGF-2 and IGF-1 were required for maximum barrier function, whereas serum increased permeability. Data are means ± SEM ($n \geq 3$). *B*) HUVEC were cultured in Transwell inserts as before and allowed to condition HIFA medium for 48h. Medium from the apical (A) or basolateral (B) chambers was concentrated and the protein content was compared to unconditioned medium by SDS-PAGE and Coomassie staining. Samples of the FGF and IGF-1 supplements where included for comparison. Most of the protein in the conditioned medium derived from these supplements. The FGF and IGF-1 supplements were replaced with highly-purified recombinant proteins to make HIFA2, which contained no detectable protein content. *C*) HUVEC were cultured to confluence in Transwell inserts and then transferred to fresh EGM-2 or HIFA2 for 24h. Cells were then fixed and stained for the junctional proteins VE-cadherin (green) and ZO-1(red). HUVEC in HIFA2 displayed more regular, linear cell-cell junctions. Scale bar = 10μm. *D)* HUVEC were grown to confluence in Transwell inserts and then transferred to HIFA2 medium. Fatty acid free BSA (0.1μg/ml) was added to either the top or bottom chambers, or to both. The concentration of BSA in both chambers after 24h was determined by SDS-PAGE and Coomassie staining. The panel shows a representative gel and quantification by densitometry. Less than 20% of the exogenous BSA crossed the monolayer in either direction over 24h. Data are means ± SEM ($n=3$).

Fig. 2 Proteomic analysis of polarized endothelial cell secretion. *A*) The apical and basolateral EC proteomes were derived from three independent experiments. The Venn diagram shows the total number of proteins detected in each case, and the overlap in identification between the three datasets. *B)* To analyze the distribution of proteins between the apical and basolateral compartments, Log2 ratios (apical/basolateral) where plotted for 840 proteins detected in two or more experiments. The majority of proteins were polarized to the apical surface. *C)* Further analysis interrogated the trafficking routes of these proteins. Conventional soluble secreted

proteins where identified from the VerSeDa as having no predicted transmembrane region and a SignalP score of >0.6. Extracellular vesicle cargoes were obtained from the EVpedia database by matching against the top 500 predicted human EV proteins. Conventional secretion was slightly biased towards the basolateral compartment, whereas EV proteins secretion was strongly biased towards the apical compartment. ECM components were identified by interrogating the Matrisome project database. These resembled the distribution of conventionally secreted proteins as a whole. *D)* Two conventionally secreted proteins were selected as representative of basolateral (Tsp1) and apical (Ang2) cargoes. The distribution between the apical and basolateral compartments predicted by TMT mass spectrometry was compared to quantification by ELISA. In both cases, the proteomic data was closely aligned to the ELISA quantification. Data are means ± SEM (n=3).

Fig. 3 Liprin-α1controls sorting of a subset of ECM proteins to the basolateral surface. *A)* HUVEC were treated with siRNAs targeting liprin-α1 and the effectiveness of silencing was determined by western blotting after 48h. All three siRNAs gave significant depletion of endogenous liprin-α1. *B)* The effect of the two most effective liprin-α1 siRNAs on EC permeability was determined by measuring the passage of FITC-dextran across the monolayer. Neither siRNA had a significant effect on permeability. Data are means ± SEM (n=3). *C)* HUVEC were treated with siRNA targeting liprin-α1 and the polarized secretion of fibronectin was quantified by ELISA of conditioned medium. Depletion of liprin-α1 had no effect on the apical secretion of fibronectin, but significantly inhibited the basolateral secretion. Data are means ± SEM (n=4); * $P<0.05$. *D)* HUVEC were treated with or without liprin-α1 siRNA and the apical and basolateral secreted proteomes were derived by TMT mass spectrometry. The vast majority of proteins showed no difference in the polarity of their secretion. A subset of proteins (red) showed a marked reduction in basolateral polarization. Conversely, a subset showed a marked reduction in apical polarization (blue).

TABLE LEGENDS

Table 1 The table shows the five most apically and five most basolaterally polarized proteins from the proteomic analysis. The most apical proteins corresponded to cargoes known to be

packaged into extracellular vesicles, whereas the most basolateral proteins were conventionally secreted ECM components. The table shows the mean ratios ± SEM (n=3).

Table 2 The table shows the identities of the proteins who markedly lose basolateral polarization on liprin-α1 depletion, in comparison to fibronectin. Also shown are the proteins who markedly lose apical polarization on liprin-α1 depletion.

Figure 1

Figure 1

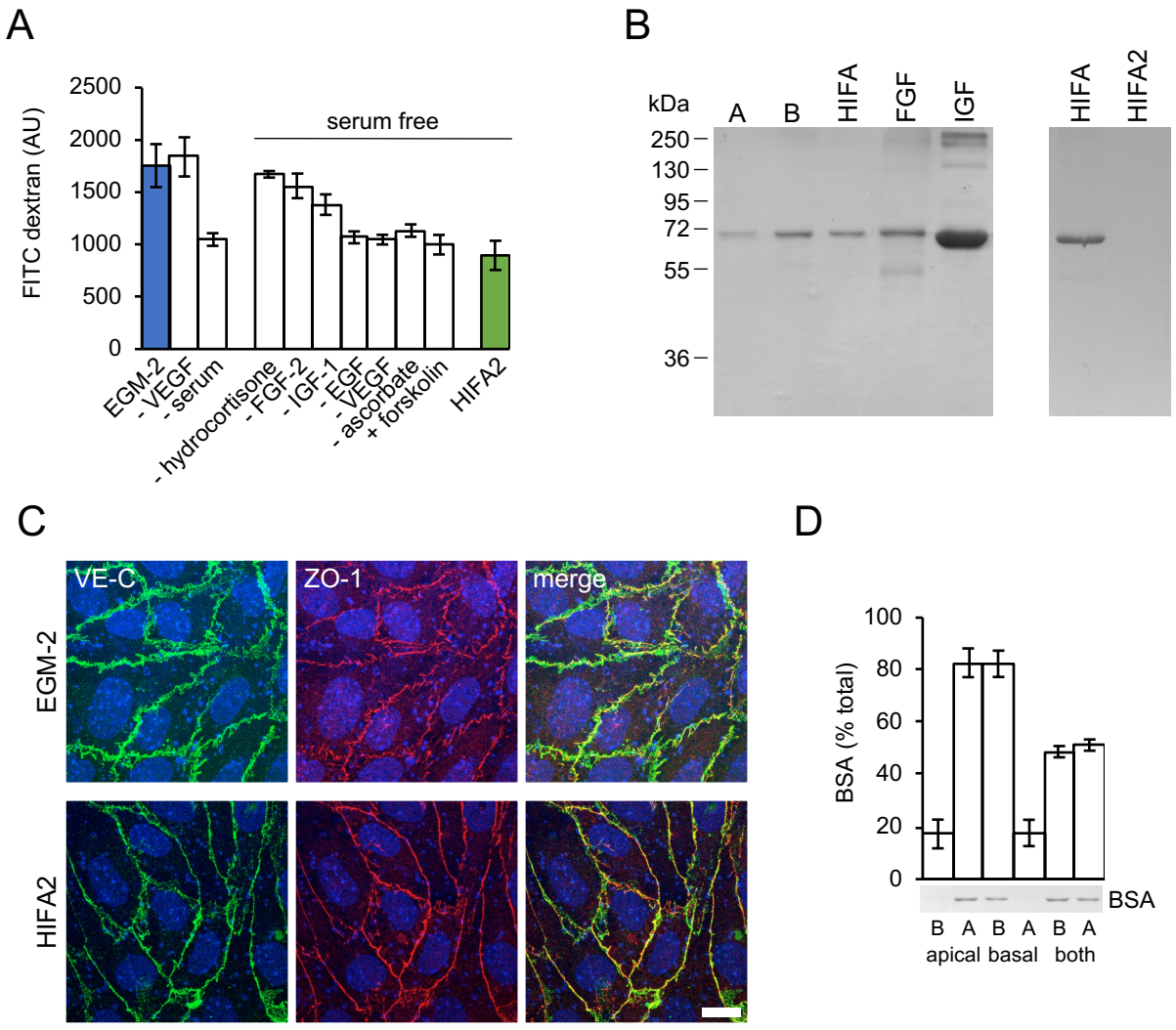

Figure 2

Figure 2

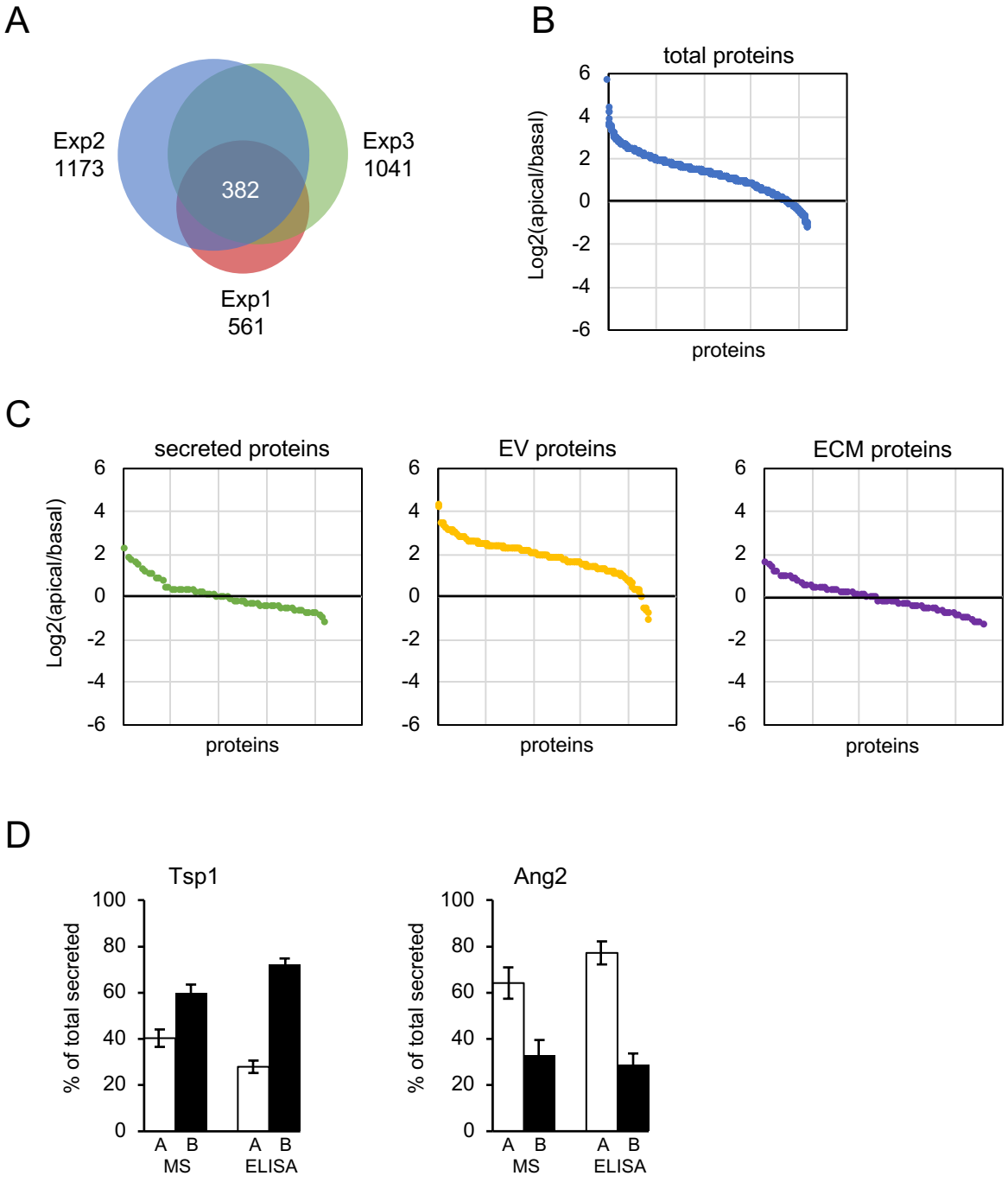

Figure 3

Figure 3

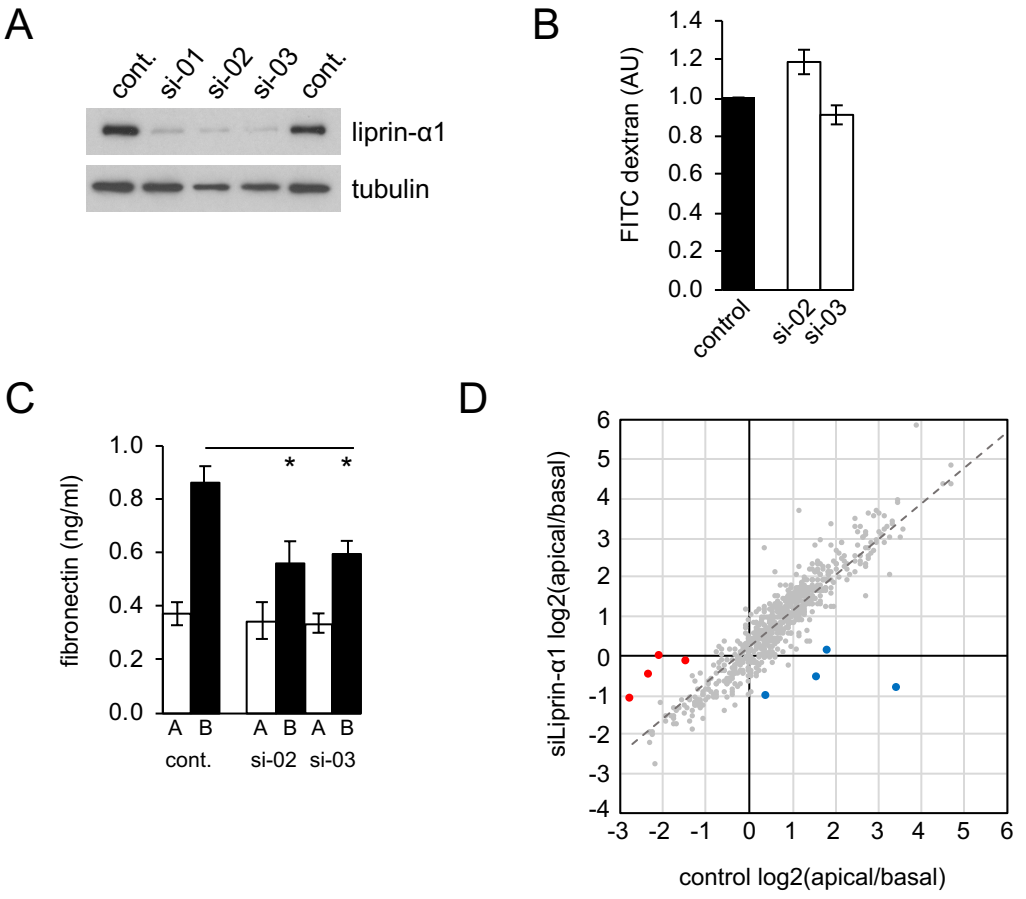

Table 1

Basolateral

Accession	Description	Ratio (A/B)	SEM
A8K7E0	Biglycan	0.424	0.033
Q13201	Multimerin-1	0.433	0.039
A0A024RAB6	Perlecan	0.438	0.026
D3DQH8	Osteonectin	0.495	0.024
A0A024R462	Fibronectin 1	0.498	0.047

Apical

Accession	Description	Ratio (A/B)	SEM
A0A0K0K1K4	Proteasome subunit alpha	6.522	0.816
P62701	40S ribosomal protein S4	6.146	1.189
Q8WVX7	Ribosomal protein S19	5.341	0.731
P25788	Proteasome subunit alpha type-3	5.090	0.683
P62195	26S protease regulatory subunit 8	4.388	0.635

Table 2

Basolateral > Apical

		control	siLiprin-α1
Accession	**Description**	**Ratio (A/B)**	**Ratio (A/B)**
A0A024R2W4	Dystroglycan-1	0.152	0.450
D0PNI2	Lysyl oxidase	0.208	0.693
B3KUE5	Phospholipase transfer protein	0.246	0.981
Q9H8L6	Multimerin-2	0.365	0.876
A0A024R462	Fibronectin 1	0.349	0.434

Apical > Basolateral

		control	siLiprin-α1
Accession	**Description**	**Ratio (A/B)**	**Ratio (A/B)**
A0A140VJI7	ECM1	1.353	0.487
A0A0S2Z3H5	Collagen I A2	3.109	0.659
Q96D15	Reticulocalbin-3	3.662	1.041
P02452	Collagen I A1	10.87	0.540

SUPPLEMENTAL TABLE LEGEND

Supplemental Table S1A The Table shows the abundance ratios (apical/basolateral) for proteomic analysis of polarized endothelial cell secretion from three independent experiments.

Supplemental Table S1B The Table shows the abundance ratios (apical/basolateral) for proteomic analysis of polarized secretion in endothelial cells treated with liprin-α1siRNA. Data are shown from three independent experiments, together with data for endothelial cells treated in parallel with an siRNA control.